[Article ID] 1003- 6326(2002)02- 0193- 07

Microstructure evolution of immiscible alloys during rapid cooling through miscibility gap①

LIU Yuan(刘 源)[1,2], GUO Jing-jie(郭景杰)[1], JIA Jun(贾 均)[1],
LI Yan-xiang(李言祥)[2], ZHAO Jiu-zhou(赵九洲)[3]
(1. School of Materials Science and Engineering, Harbin Institute of Technology, Harbin 150001, China;
2. Department of Mechanical Engineering, Tsinghua University, Beijing 100084, China;
3. Institute of Metal Research, The Chinese Academy of Science, Shenyang 110015, China)

[Abstract] A numerical model was developed to describe the coarsening of the second phase droplets under the common action of nucleation, diffusional growth and Brownian collision between minority phase droplets during rapidly cooling a hypermonotectic alloy through its miscibility gap. The simulated results show that Brownian motion is an important factor influencing the coarsening process. A faster cooling rate leads the supersaturation of the matrix liquid and the nucleation rate to grow up to a higher level, but leads to a smaller droplet radius and a higher number density. This model is used to predict the microstructural evolution of melt-spun Al-30% In ribbon. The model reflects the real physical processes well and is expected to be applicable to other immiscible alloys or other preparing processes.

[Key words] immiscible alloy; coarsening of second phase; numerical model
[CLC number] TG 146.1 [Document code] A

1 INTRODUCTION

The phase diagrams of immiscible alloys are characterized by the presence of a miscibility gap—a region in which two liquid phases co-exist in equilibrium, as depicted in Fig. 1. If such a homogeneous, single phase liquid is cooled into the miscibility gap, it will decompose into two liquids (L1 and L2). Generally, the liquid-liquid decomposition starts with nucleation of the minority phase in the form of droplets. These droplets grow by diffusion of solute in the matrix. They can also settle or float due to the action of gravity (Stokes motion), also can migrate due to a temperature or concentration gradient (Morangoni motion). The solidified microstructure strongly depends on all these processes. There have been several attempts to model at least parts of the microstructure evolution in the miscibility gap. Rogers and Davis[1], Markworth and Gelles[2] treated the collision and coagulation statistics of droplets. Fredriksson and his co-workers[3,4], Ahlborn et al[5] and Uebber et al[6] have analyzed the microstructure evolution of Zn-Bi, Al-Pb and Zn-Pb, respectively. Ratke et al[7] also analyzed the problem under the common action of nucleation, growth and Stokes settlement for a system of constant temperature and constant supersaturation, by assuming that the alloy was instantaneously cooled to a temperature just above the monotectic reaction and then calculating the phase separation kinetics under the condition of constant thermophysical properties, constant supersaturation specified. Zhao[8] established a numerical model based on variational thermophysical properties and supersaturation during a real continuously cooling process, but he also neglected the influence of collision between droplets.

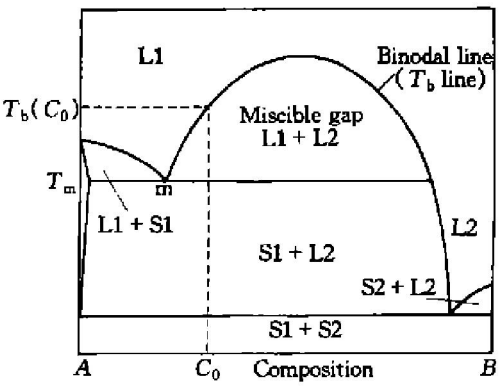

Fig. 1 Schematic phase diagram of immiscible system

Research in the last decades showed that a fine dispersion of minority phase particles in a hypermonotectic alloy can be obtained by rapidly quenching or cooling the melt through the miscibility gap[9~11]. The applied methods include gun method, melt spinning, planar flow casting as well as a modified planar flow casting method etc. In these cases, the liquid-liquid decomposition takes place while the temperature continuously decreases. The thermophysical properties, supersaturation as well as the nucleation rate of minority phase droplets change accordingly. In

① [Foundation item] Project (9- 04) supported by Emerson Foundation of USA
[Received date] 2001- 08- 07; [Accepted date] 2001- 09- 17

this paper, we will develop a numerical model to simulate the microstructure evolution allowing all thermophysical properties, supersaturation to vary with temperature and thus with time. This model considers the common action of nucleation, diffusional growth and Brownian collision between minority phase droplets, neglecting Stokes sedimentation or Marangoni motion because the minority phase droplets are very fine and their staying time in the miscibility gap is as short as 10^{-4}~ 10^{-3}s. The model will be used to predict the microstructure evolution of melt spun Al-In immiscible alloys.

2 FORMULATION OF MODEL

2.1 Nucleation

Generally, classical nucleation theory can be used to predict the nucleation of the minority phase droplets in the liquid metallic matrix[12]. The homogeneous nucleation rate is given by

$$I_{\hom} = NO\Gamma Z\exp(-\Delta G_c/k_BT) \quad (1)$$

where $N = (x_A\Omega_A + x_B\Omega_B)^{-1}$, $O = 4n_c^{2/3}$, $\Gamma = 6D_{In}/\lambda$, $Z = (\Delta G_c/3\pi k_BTn_c^2)^{1/2}$, $\Delta G_c = 16\pi\sigma^3/(3\Delta G_V^2)$. In these equations, N is the number density of atoms per volume. Ω_A, Ω_B are the atomic volumes of A and B components. x_A, x_B are the mole fraction of component A and B. n_c is the number of atoms in a droplet with critical radius R^* ($= 2\sigma/\Delta G_V$). σ is the interfacial tension between the two liquids. ΔG_V is the gain in free energy per volume on nucleation. D_{In} is the diffusion coefficient of In element. λ is the average jump distance of a solute atom due to diffusion. k_B is Boltzmann's constant. T is absolute temperature and ΔG_c is the energy barrier for nucleation.

2.2 Diffusion controlled growth of droplets

The droplets in a supersaturated matrix will grow or shrink by diffusional transport of solute in the matrix. The growth or shrinkage rate can be expressed as[8]

$$v(R,t) = \frac{dR}{dt} = D_{In}\frac{C_m(t) - C_I(R,t)}{C_\beta(t) - C_I(R,t)}\frac{1}{R} \quad (2)$$

where $C_m(t)$ and $C_\beta(t)$ are the mean field concentration of solute B in the matrix liquid and in the droplets; $C_I(R,t)$ is the concentration of solute B in the matrix at the interphase boundary and R is the droplet radius. We assume that the interface of a growing droplet is always in local equilibrium and its composition shall depend on droplet radius according to the Gibbs-Thomson relation:

$$C_I(R,t) = C_\infty(t)\exp(\alpha_s/R) \quad (3)$$

where $\alpha_s = 2\sigma\Omega_d/k_BT$ is the capillary length and $C_\infty(t)$ is the equilibrium composition at a flat interface boundary at time t. Ω_d is the average atom volume in the droplet. It can be found from Eqn. 2 that, if $C_m(t) > C_I(R,t)$, $v(R,t) > 0$, it implies that the droplets with the radius R continuously grow; if $C_m(t) < C_I(R,t)$, $v(R,t) < 0$, it implies that the droplets with the radius R continuously diminish. In other words, this equation also reflects the Ostwald ripening process of droplets.

2.3 Population dynamics

The growth behavior of a polydispersed system of droplets can be described by defining a droplet radius distribution function $f(R,t)$. Then $f(R,t)dR$ is the number of droplets with radius in the range of R and $R + dR$ per unit volume. If we consider the common action of the nucleation, the diffusional growth and the collisions between droplets, the distribution function then obeys a continuity equation of the following form[8].

$$\frac{\partial f(R,t)}{\partial t} = \frac{\partial I_{\hom}}{\partial R}\bigg|_{R=R^*} - \frac{\partial}{\partial R}[v(R,t)\cdot f(R,t)] + \left[\frac{1}{2}\int_0^R W(R_1,R_2)f(R_1,t)f(R_2,t)\cdot\left[\frac{R}{R_2}\right]^2 dR_1 - \int_0^\infty W(R,R_1)f(R,t)f(R_1,t)dR_1\right] \quad (4)$$

in which

$$R_1^3 + R_2^3 = R^3$$

In the right of this equation, the first, the second and the third terms describe the creation of droplets with radius of R due to the nucleation, the diffusional growth and the collisions between droplets, respectively. $W(R_1,R_2)$ is the so-called integrated collision volume measured in units of cubic metres per second. For Brownian collision between droplets, $W(R_1,R_2) = 8R_1k_BT/3\eta R_2$ in which η is the kinetic viscosity of the matrix liquid phase.

The mean concentration $C_m(t)$ in the matrix liquid changes with time. According to solute conservation, we can obtain

$$C_0 = \Phi(t)C_\beta(t) + [1-\Phi(t)]C_m(t) \Rightarrow$$
$$C_m(t) = [C_0 - \Phi(t)C_\beta(t)]/[1-\Phi(t)] \quad (5)$$

where $\Phi(t)$ is the time-dependent volume fraction of the minority phase. It can be expressed as

$$\Phi(t) = \frac{4}{3}\pi\int_0^\infty R^3f(R,t)dR \quad (6)$$

The droplet distribution function during liquid-liquid decomposition is determined via a solution to Eqns. (1), (2) and (4).

2.4 Temperature evolution

The single roller melt spinning rapid solidification can be simplified as a one-dimensional (in the direction normal to the wheel substrate surface), two-phase (solid and liquid), heat transfer problem (i.e., a Stefen problem) that has changing conditions at the moving boundary (as illustrated in Fig. 2). A fi-

nite difference model, neglecting the convective heat transfer, was set up to describe this kind of one-dimensional heat transfer:

$$\frac{\partial T}{\partial t} = \frac{1}{c_p}\frac{\partial}{\partial x}\cdot\left[K\frac{\partial T}{\partial x}\right] + \frac{Q}{c_p} \tag{7}$$

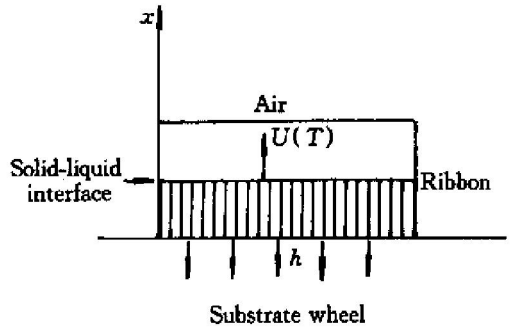

Fig. 2 Diagram of physical model for substrate rapid solidification

where Q is a heat source term. c_p is the specific heat ($J\cdot m^{-3}\cdot K^{-1}$) of alloy. K is the thermal conductivity ($W\cdot m^{-2}\cdot K^{-1}$). The appropriate equation, expressed in finite difference form to give the change in temperature of the jth element, is thus

$$\delta T_j = \delta t \cdot \left[\frac{1}{c_p}\left[\frac{\partial K}{\partial x}\right]\left[\frac{\partial T}{\partial x}\right] + \frac{K}{c_p}\left[\frac{\partial^2 T}{\partial x^2}\right] + \frac{Q^*}{c_p} + \frac{q_i}{c_p \delta x}\right] \tag{8}$$

where the superscript * represents the solidification front. The subscript i represents the interface including melt/substrate interface and melt/air interface. The boundary conditions are as follows:

$$Q^*|_{j=j^*} = U\Delta H_f/\delta x : Q^*|_{j\neq j^*} = 0 \tag{9}$$

$$q_i|_{j=j_i} = \begin{cases} h_{\text{eff}}(T_i - T_w) & \text{At melt/substrate interface} \\ 0 & \text{At melt/air interface} \end{cases}$$

$$q_i|_{j\neq j_i} = 0 \tag{10}$$

$$\left.\frac{\partial K}{\partial x}\right|_{j=j^*} = \frac{K_L - K_S}{2\delta x} : \left.\frac{\partial K}{\partial x}\right|_{j\neq j^*} = 0 \tag{11}$$

In these equations, h_{eff} is the effective heat transfer coefficient at melt/substrate interface ($W\cdot m^{-2}\cdot K^{-1}$). T_w and T_a is the wheel temperature and the air temperature, respectively. The growth rate U can be written as[13]

$$U(\Delta T) = \frac{D_{Al}}{a}\left[1 - \exp\left[-\frac{\Delta H_f(T_L - T)}{RTT_L}\right]\right] \tag{12}$$

where R is the gas constant. ΔH_f is the molar enthalpy of fusion and T_L is the liquidus of Al. D_{Al} is the diffusion coefficient of Al element in the liquid. a is the effective molecular jump distance.

3 SIMULATED RESULTS OF Al-30%In AND DISCUSSION

The calculation proceeded as follows: We firstly simulate the temperature evolution in the ribbon, therefore obtain the staying time t' of the melt in the miscibility gap and the corresponding average cooling rate $\dot{T}$ at different positions. Then we assume that the initially homogeneous hypermonotectic alloy melt is uniformly cooled down from the coexisting temperature T_b with the corresponding cooling rate $\dot{T}$ until the time increases up to t' at a time step dt. At the beginning of each time step, the supersaturation ($C_m(t) - C_\infty(t)$) and the mean concentration of solute in the matrix liquid and the nucleation rate of the minority phase, the numbers of the droplets as well as the average droplet radius are calculated. It is assumed that the original radius of the nucleus is the critical radius R^*.

The phase diagram and the thermodynamical data come from Ref. [14]. The interfacial tension, $\sigma_{L1L2}(T)$, comes from the fitted experimental values in Ref. [15]:

$$\sigma_{L1L2}(T) = 0.508(1 - T/1112)^{1.73} \tag{13}$$

The diffusion coefficient of In, D_{In}, in the matrix liquid is estimated as $3.9\times10^{-9} m^2 s^{-1}$ at monotectic temperature. It is related to temperature as follows[16]:

$$D_{In}(T) = D_0 T^2 \tag{14}$$

D_0 is a constant that can be determined from the diffusion coefficient at the monotectic temperature.

3.1 Temperature evolution

Fig. 3 shows the temperature evolution in a 100 μm thick Al-30% In ribbon and the corresponding average cooling rate of different positions as well as the staying time of the melt in the miscibility gap. Due to the release of the latent heat, the temperature gradient before the solidification front declines even a flat temperature distribution occurs in the later stage of the solidification process. With increasing distance from the chilled surface, the staying time of the melt increases, while the average cooling rate decreases.

3.2 Microstructure evolution at constant cooling rate

We now consider the situation of cooling a hypermonotectic alloy melt (Al-30% In) continuously through the miscibility gap with three processes running concurrently: nucleation, diffusional growth or shrinkage and Brownian collision. Fig. 4 shows evolution of the supersaturation of solute in the matrix liquid and the homogeneous nucleation rate of the minority phase at a cooling rate of $2.43\times10^4 K/s$ (in the middle part of the ribbon with 100 μm in thickness). The applied average cooling rate and the staying time come from Fig. 3(b). Fig. 4 clearly demonstrates that, with cooling through the miscibility gap, the supersaturation continuously increases until it reaches a critical amount such that nucleation starts.

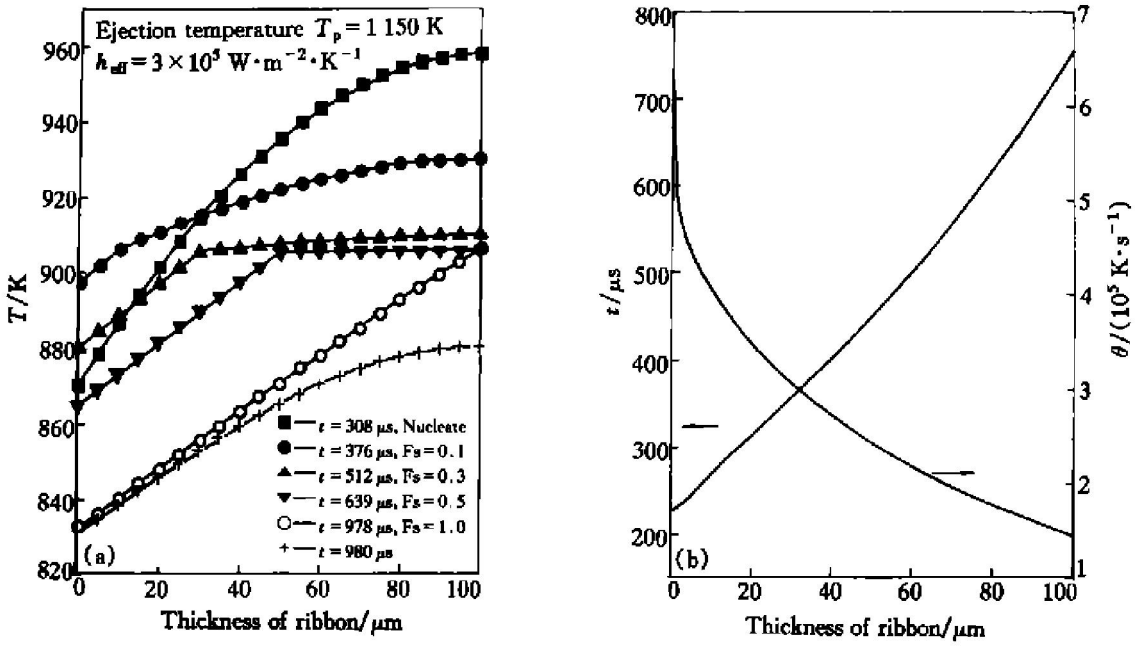

Fig. 3 Temperature evolution in 100 μm thick Al-30% In ribbon (a) and corresponding average cooling rate ($\dot{\theta}$) and staying time (t) in miscibility gap through thickness (x) (b)

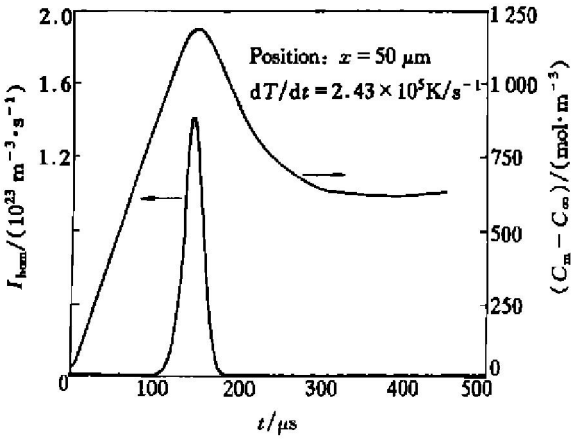

Fig. 4 Supersaturation of solute ($C_m - C_\infty$) in matrix liquid and nucleation rate (I_{hom}) of minority phase against time (t) at cooling rate of 2.43×10^4K/s

Then the supersaturation does not directly decrease but increases further for a short time before it reaches a maximum value. This effect is the result of the common action of two opposing processes: nucleation and diffusional growth decrease the supersaturation and the continuous decrease of the temperature increases it in as much as the binodal line varies with temperature (see the phase diagram in Fig. 1). Let $\Delta C = C_m(t) - C_\beta(t)$ be a measure of the supersaturation, then Eqn. (5) can be changed into:

$$\frac{d\Delta C}{dt} = -\frac{dC_\infty}{dT}\frac{dT}{dt} - \frac{d\phi}{dt}\frac{1}{1-\phi}(C_\beta - C_m) - \frac{\phi}{1-\phi}\frac{dC_\beta}{dT}\frac{dT}{dt} \quad (15)$$

Considering that the volume fraction of the minority phase is very low, especially during the period of nucleation, and dC_β/dt is also small even when the temperature is close to the monotectic reaction, we can obtain the following Eqn. (16) inserting $\phi(t) = 4\pi\langle R\rangle^3 n(t)/3$ ($\langle R\rangle$ is the average droplet radius, $n(t)$ is the number density of droplets) into Eqn. (15):

$$\frac{d\Delta C}{dt} = -\frac{dC_\infty}{dT}\frac{dT}{dt} - \frac{4\pi}{3}\langle R\rangle^2 \left[\langle R\rangle\frac{dn}{dt} + 3n(t)\frac{d\langle R\rangle}{dt}\right](C_\beta - C_m) \quad (16)$$

During the early period of the liquid-liquid decomposition, the supersaturation of solute in the matrix liquid increases because both the nucleation rate I and the number density of droplets n are too small. So the supersaturation is primarily dependent on the first term in the right side of Eqn. (16). Therefore the supersaturation rises with decreasing temperature. The enhancement of the supersaturation leads to a rapid increase of the nucleation rate and therefore the number density of droplets increase rapidly. When the nucleation rate, also the number density of droplets increases up to a maximum value, the rise of the second term in the right hand of Eqn. (16) leads the supersaturation to decrease. At the same time, the diffusional growth of the minority phase droplets also leads to the decrease of the supersaturation.

The number density of droplets is shown in Fig. 5 together with the average droplet radius. In the early stage of the cooling process, the number density of droplets increases continuously with increasing nucleation rate. At this time, although Brownian collision between droplets also brings on the drop of the number density, compared with the effect of nucleation rate, its effect is slightly so that the number density increases. But when the number density increases up to a maximum value, the newly nu-

cleated droplets can not offset the decrease of the droplet number due to strong Brownian collision between droplets, so as shown in Fig. 5, the number density decreases with time. The rise of mean droplet radius is the result of common action of two processes: the diffusional growth and Brownian collision between droplets. In the early stage of the cooling process, due to the slightly Brownian collision, so the diffusional growth is the primary factor leading to the rise of mean droplet radius. But in the later stage of the cooling process, Brownian collision becomes stronger. Therefore the rise of mean droplet radius is the result of common action of the diffusional growth and Brownian collision between droplets.

Fig. 6 shows the evolution of the normalized ra-

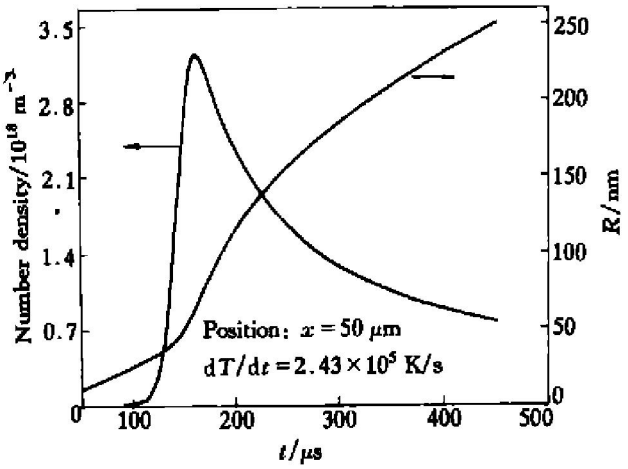

Fig. 5 Droplet number density and average radius against time in middle part of 100 μm thick Al-30% In ribbon

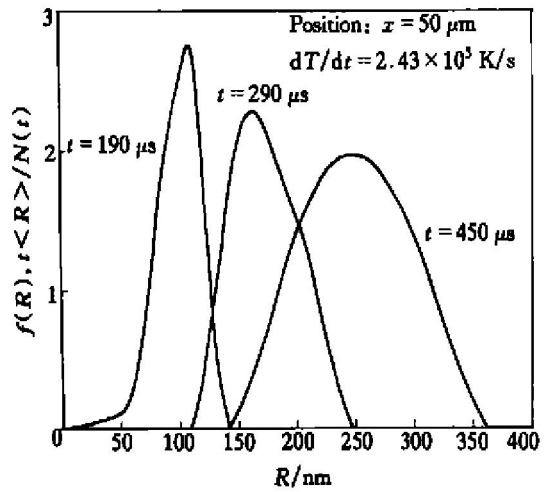

Fig. 6 Evolution of radius distribution of droplets in middle part of 100 μm thick Al-30% In ribbon

dius distribution of droplets during the cooling process. It can be found that all of the curves are not symmetrical due to the diffusional growth and Brownian collision between droplets. With time proceeded, the radius distribution curve moves from the left (low droplet radius) to the right (high droplet radius) and the width of the radius distribution increases.

3.3 Influence of cooling rate on microstructure evolution

Because the cooling rate is different at different height of the ribbon, so the real aim is to find the microstructure evolution through the thickness of hypermonotectic Al-In ribbons. In the following discussion, we define a dimensionless time $\theta = t/t'$. $\theta = 1$ denotes that the liquid-liquid decomposition process finishes. Fig. 7 shows the influence of cooling rate on the nucleation rates and the supersaturations of solute in the matrix liquid when a 100 μm thick Al-30% In ribbon is cooled through the miscibility gap. In the downside of the ribbon ($x = 10$ μm), a faster cooling rate about 4.02×10^4 K/s leads the supersaturation and also the nucleation rate to increase up to a higher level. With increasing distance from the chilled surface, for example, in the middle part ($x = 50$ μm) and the upside ($x = 90$ μm) of the ribbon, the reached supersaturation and nucleation rate decrease because of the lower cooling rates there. The faster the cooling rate, the higher the nucleation rate and the shorter the incubation time of nucleation. Besides this expected effect, the shape of all curves of the supersaturation and also that of all curves of nucleation rate are very similar.

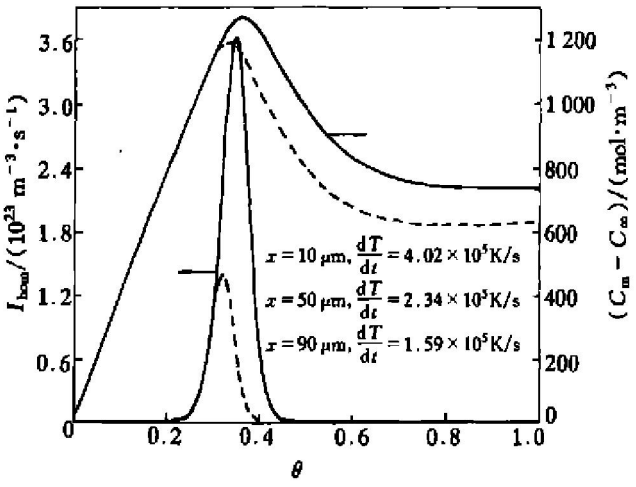

Fig. 7 Influence of cooling rate on nucleation rate of minority phase and supersaturation of solute ($C_m - C_\infty$) in matrix liquid

Fig. 8 shows evolutions of average droplet radius under different cooling rates. We can find from it that, a faster cooling rate leads to a smaller average droplet radius. It is because that a faster cooling rate shortens the time for the diffusional growth and Brownian collision between droplets.

Because there exists a continuous change of the cooling rate through the thickness of the ribbons prepared with melting spinning process or strips with other rapid quenching processes, undoubtedly, a continuous change of the average droplet radius is inevitable. For a 100 μm thick Al-30% In ribbon the evolution of the average droplet radius, together with

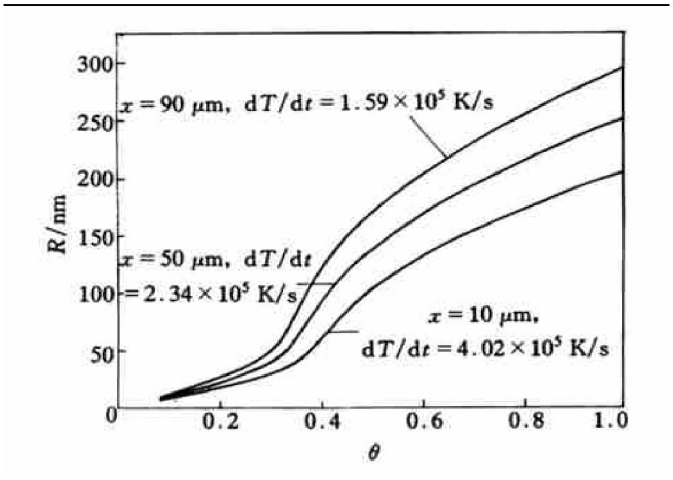

Fig. 8 Evolution of average droplet radius with time at various cooling rates

the number density of droplets through the thickness is shown in Fig. 9. It is obvious that, with increasing distance from the chilled surface (with decreasing cooling rate), the average droplet radius increases due to a longer time for the diffusional growth and Brownian collision between droplets. But the number density decreases due to a decreasing nucleation rate and a longer time for Brownian collision.

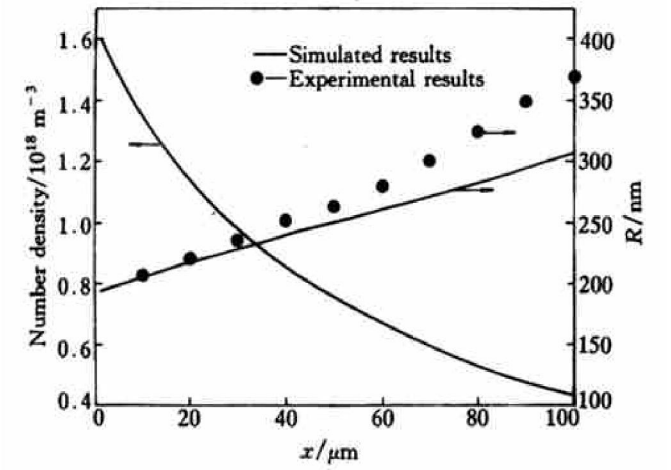

Fig. 9 Evolution of average radius (R) and number density of droplets through 100 μm thick Al-30% In ribbon

4 EXPERIMENTAL RESULTS

An Al-30% In alloy charge of approximately 30 g made up of 99.99% pure aluminum and indium are induction melted in quartz crucible under a dynamic argon atmosphere, held for 300 s at 1 150 K and ejected with an argon overpressure of 80 kPa through a 12 mm diameter nozzle onto the outer surface of a polished copper wheel rotating with a tangential speed in the range 10~ 40 m/s. The ribbons are typical 40~ 200 μm in thickness, 7~ 9 mm in width. A ribbon about 100 μm in thickness is selected to test whether the model has a certain predictive capabilities. A typical back-scattered electron images of the cross-section of the selected ribbon is shown in Fig. 10. The evolution of the measured average droplet radius through the thickness is shown in Fig. 9. The difference between the experimental results and the simulated ones is slight in the downside of the ribbon but rises with increasing distance from the chilled surface. It is maybe because the bigger droplets in the upside of the ribbon induce gravitation coagulation. In addition, the pushing action of the solidification front also causes the situation. Although there exist some differences between the simulated results and the experimental ones, the general trend is correct and the agreement is satisfactory in view of the influence of many complex factors.

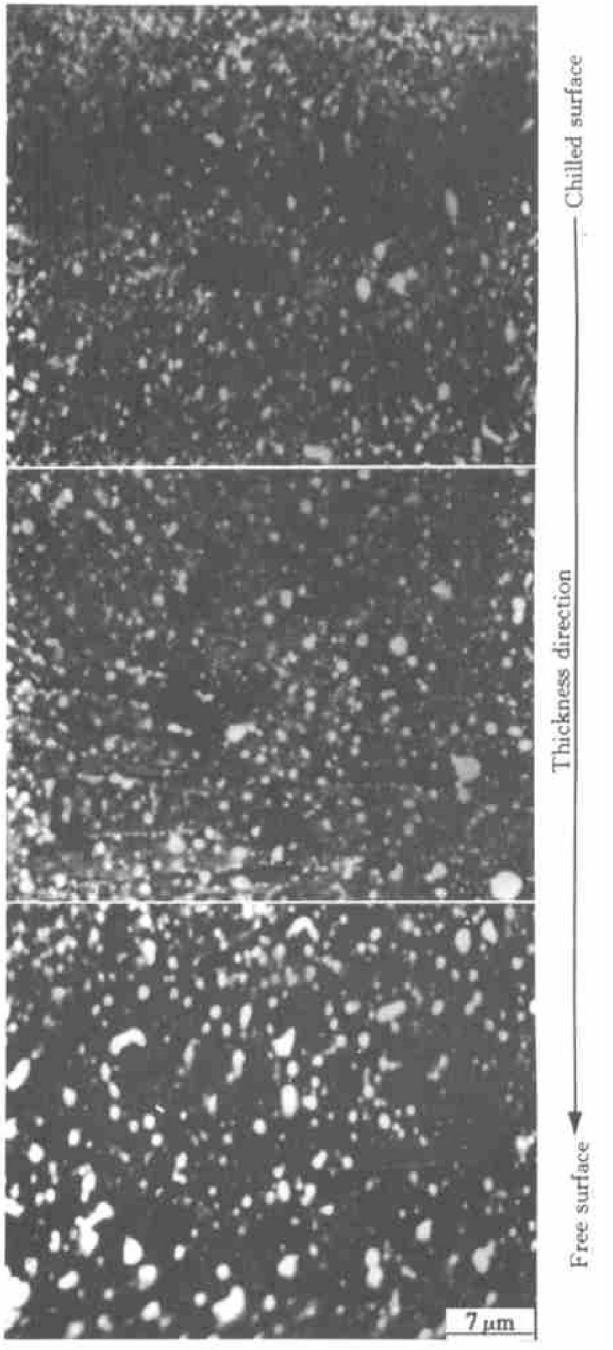

Fig. 10 Typical back-scattered electron images of cross-section of selected 100 μm thick Al-30% In ribbon

Although our model has some predictive capabilities in a certain degree, we are convinced that a further improvement of the model could not be made unless the motion of droplets, effects of convective diffusion on the growth, collision and coagulation of droplets caused by Stockes motion and Morangni migration, pushing action of the solidification front etc, are taken into consideration. At the same time, the effect of the motion of droplets on the concentration and temperature field is also considered. In addition, the accurate thermophysical properties of the alloys investigated are necessary.

5 CONCLUSION

A numerical model has been developed to describe the microstructural evolution under the common action of nucleation, diffusional growth of the minority phase droplets as well as Brownian collision between them during rapid cooling a hypermonotectic alloy through the miscibility gap. At a constant cooling rate, the number density of droplets increases continuously because of the increasing nucleation rate. But when the number density increases up to a maximum value, the newly nucleated droplets can not offset the decrease of the droplet number due to Brownian collision between droplets, the number density decreases with time. The rise of mean droplet radius is the result of common action of diffusional growth and Brownian collision between droplets. It continuously increases with time. The calculated results show that a faster cooling rate leads the supersaturation of solute in the matrix liquid and also the nucleation rate of the minority phase to increase up to a higher level, but leads to a smaller droplet radius. For ribbons, with increasing distance from the chilled surface, the cooling rate decreases and the mean droplet radius increases. The comparison between the calculated results and the experimental ones shows that the model is feasible for predicting the coarsening of the second phase during rapidly cooling an immiscible alloy through its miscibility gap.

[REFERENCES]

[1] Rogers J, Davis R. Modeling of collision and coalescence of droplets during microgravity processing of Zn-Bi immiscible alloys [J]. Metall Trans A, 1990, 21: 59- 64.

[2] Markworth A J, Gelles S H. Microgravity studies in the liquid phase immiscible system Al-In [A]. Computer Simulations for Materials Application [C]. R Arsenault, J Beler and J. Simmons (Gaitherburg: NBS), 1976. 1023- 1036.

[3] Bergman A, Carlberg T, Fredriksson H. A study of the coalescence process inside the miscibility gap in Zn-Bi alloy [A]. Materials Processing in the Reduced Gravity Environment of Space [C]. ed G. E. Rindone (Amsterdam: Elsevier), 1982. 579- 592.

[4] Carlberg T, Fredriksson H. The influence of microgravity on the solidification of Zn-Bi immiscible alloys [J]. Metall Trans A, 1980(11): 1665- 1676.

[5] Ahlborn H, Neumann H, Schott H J. Segregation behavior of rapidly cooled monotectic Al-In and Al-Pb alloys [J]. Z Metall, 1993, 84(11): 748- 754.

[6] Uebber N, Ratke L. Undercooling and nucleation within the liquid miscibility gap of Zn-Pb alloys [J]. Scr Metall Mater, 1991, 25: 1133- 1137.

[7] Alkemper J, Ratke L. Concurrent nucleation, growth and sedimentation during solidification of Al-Bi alloys [J]. Z Metall, 1994, 85: 365- 371.

[8] Zhao J Z, Ratke L, Feuerbacher B. Microstructure evolution of immiscible alloys during cooling through the micibility gap [J]. Model Simul Mater Sci Eng, 1998(6): 123- 139.

[9] Chattopadhyay K, Ramachandrarao P. Rapid solidification and decomposition of a hypomonotectic Al-Cd alloy [J]. J Mater Sci, 1980, 15: 685- 692.

[10] Goswami R, Chattopadhyay K. Microstructural developments in rapidly solidified monotectic alloys [J]. Mater Sci Eng, 1994, A179/A180: 163- 167.

[11] Berrenberg T, Sahm P R. Production and properties of a hypermonotectic Al-Pb alloy as an antifriction layer, Part Ⅰ: Rapidly solidified cast coating [J]. Z Metallkde, 1996, 87: 187- 190.

[12] Granasy L, Ratke L. Homogeneous nucleation within the liquid miscibility gap of Zn-Pb alloys [J]. Scr Metall Mater, 1993, 28: 1329- 1334.

[13] Ostlund A, Fredriksson H, Fredriksson H. State of the Art Simulation of Casting and Solidification Processes [M]. Strasbourg: European Materials Research Society, 1986. 145- 152.

[14] Sommer F, Krull H G, Yu S K. Immiscible Liquid Metals and Organic [M]. DGM Informations GesellschaftmbH, 1993. 79.

[15] Merkwitz M, Hoyer W. Liquid-liquid interfacial tension in the demixing metal systems Al-Pb and Al-In [J]. Z Metallkd, 1999, 90(5): 363- 369.

[16] Zhao J Z, Ratke L. Kinetics of phase separation in a hyperminotectic Al-Pb alloy [J]. Z Metallkd, 1998, 89: 241- 245.

(Edited by HUANG Jin-song)